Grabalosa Saubí, Jordi; Ferrer Real, Inés; Martínez-Romero, Oscar; Elías-Zúñiga, Alex; Plantá, X.; Rivillas, F. (2016). "Assessing a stepped sonotrode in ultrasonic molding technology. Universitat". *Journal of Materials Processing Technology*, vol. 229, p. 687-696

The published journal article is available online at:
http://dx.doi.org/10.1016/j.jmatprotec.2015.10.023

Assessing a stepped sonotrode in ultrasonic molding technology

J. Grabalosa [a,*], I. Ferrer [a], O. Martínez-Romero [b], A. Elías-Zúñiga [b], X. Plantá [c,d], F. Rivillas [d]

[a] Department of Mechanical Engineering and Civil Construction, Universitat de Girona, Av. Lluis Santaló s/n, 17071 Girona, Spain
[b] Escuela de Ingenieria y Ciencias, Tecnologico de Monterrey, Campus Monterrey, Ave. Eugenio Garza Sada 2501, Monterrey, NL 64849 Mexico
[c] Fundació EURECAT, Parc Tecnològic del Vallès, Av. Universitat Autònoma 23, E-08290, Cerdanyola del Vallès, Barcelona, Spain
[d] Ultrasion S.L., Parc Tecnològic del Vallès, Av. Universitat Autònoma 23, E-08290, Cerdanyola del Vallès, Barcelona, Spain

a b s t r a c t

Ultrasonic molding is a new technology used to process polymeric micro-molded parts. An ultrasonic horn, or sonotrode, transmits ultrasonic energy which melts the material and pushes it into a mold cavity to configure a shape. Sonotrode design – and any transformations to the dimensions or shape caused by tool wear – strongly affects efficient operation. The sonotrode may go beyond the generator operating frequency range, thus affecting process performance. This paper assesses two issues involving a stepped sonotrode employed in ultrasonic molding: (i) a design procedure that can predict the sonotode's behavior during the molding process and (ii) a method for creating a sonotrode operating frequencies map which will facilitate the design of new sonotrodes and be able to determine the extent to which they can be re-machined after a certain period of wear. Numerical simulations carried out by finite element methods were compared to experimental measurements performed to capture the sonotrode frequency vibrational modes. A frequency map provides the dimensional range within which the sonotrode can be re-machined in order to eliminate tool wear and allow the sonotrode to work properly again, thus extending the lifecycle of the tool.

1. Introduction

Ultrasonic energy is currently being used to manufacture various components (Sackmann et al., 2015) with processes such as ultrasonic welding (Rani and Rudramoorthy, 2013) and ultrasonic machining (Singh and Khamba, 2006). It is also used to assist during the manufacturing process such as, for example, in ultrasonic-assisted EDM (Liew et al., 2014), ultrasonic-assisted machining (Tabatabaei et al., 2013) and ultrasonic assisted injection molding (Yang et al., 2014). According to Michaeli and Opfermann (2006), technologies based on ultrasound are also becoming an attractive alternative that can improve the micro injection process for obtaining micro parts weighing less than 10 mg.

Ultrasonic molding is a new technology for processing polymeric materials, using ultrasonic vibration energy to melt the material and fill the mold cavity. In this process the plastic pellets are introduced directly inside the plasticization chamber and the material melts due to the ultrasonic energy applied by the sonotrode. The sonotrode also acts as a plunger, pushing the molten material inside the mold cavity. This process is divided into four stages, as illustrated in Fig. 1. First, the pellets are introduced into the plasticization chamber (Fig. 1(a)). Then, the sonotrode is introduced until the tip reaches the pellets (Fig. 1(b)). Next, the sonotrode starts to vibrate and move down applying compression force to the pellets (Fig. 1(c)). According to Michaeli et al. (2011), the pellets melt because the sonotrode vibrational energy increases their internal heat and the friction between them. The molten material starts to flow through the runners inside the mold cavity. When the mold cavity is filled up, the sonotrode remains in its final position to maintain the pressure during the material cooling stage (Fig. 1(d)). Finally, the sonotrode returns to its initial position and the mold is opened to extract the molded part.

Michaeli et al. (2002) carried out pioneering tests using ultrasonic energy rather than common heat energy to increase the efficiency when plasticizing small amounts of polymeric materials. They subsequently showed the feasibility of ultrasonic plasticizing of polymeric materials in different micro parts of Polypropylene (PP) and Polyoxymethylene (POM) using a conical sonotrode working at 20,000 Hz (Michaeli and Opfermann, 2006). The results

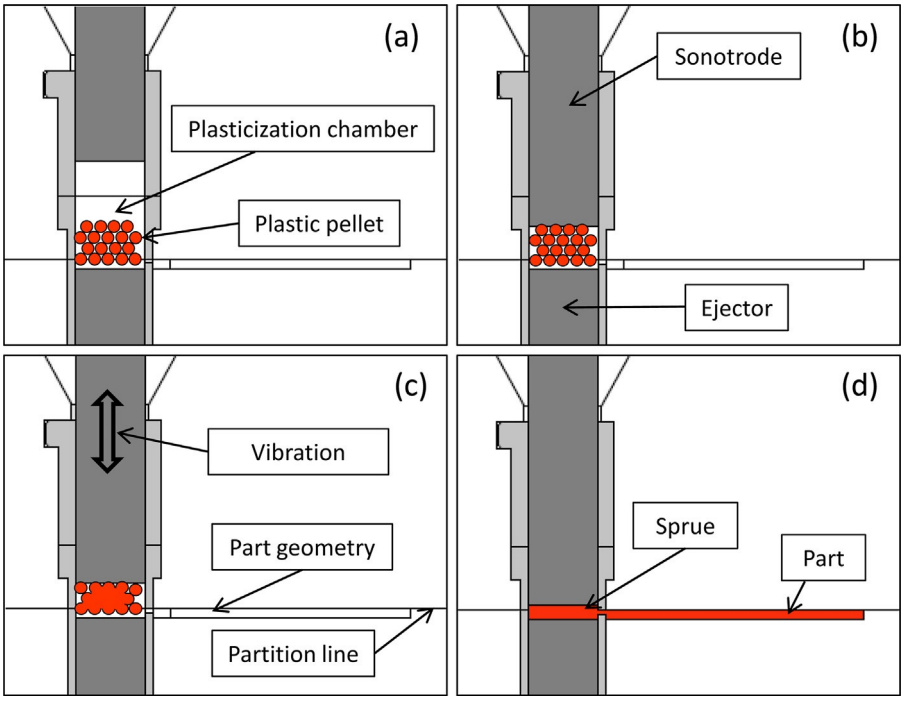

Fig. 1. Phases of the ultrasonic molding process: (a) feeding, (b) vibration initiation, (c) plasticization and cavity filling and (d) packing and cooling.

presented showed the potential use of ultrasonic energy as an alternative to conventional processes.

Ultrasonic energy is also used to assist injection molding process during the filling and packing stages. In that case, a conventional machine is used to inject the molten material into a mold cavity and next a sonotrode included in this cavity provides ultrasonic vibration to the final part before the molten material is solidified to improve the part properties. Yang et al. (2014) used a 45 mm diameter horn, vibrating at 20,000 Hz with and 15 microns of amplitude to investigate the influence of the vibration energy when processing polycarbonate flat specimens. Results showed an improvement of the filling efficiency, because the melt temperature could be maintained higher than in conventional injection molding during the filling stage. Sato et al. (2009) used a 19,000 Hz and 11 microns of amplitude acoustic equipment to process polycarbonate parts. They found that ultrasonic vibration enhanced the replication capabilities of the process, in particular, the weight was increased and surface roughness was improved.

In ultrasonic molding technology, the ultrasonic energy melts the entire material and, at the same time, the sonotrode pushes it into the mold cavity (Fig. 1(c) and (d)), which differs completely of assisted injection molding process. Ultrasion S.L. (Sirera et al., 2012) implemented this technology industrially with a machine called Sonorus 1G, obtaining successful results on process efficiency and reduced energy consumption compared to conventional processes of micropart production. Thus far, stepped sonotrodes have been used in Sonous 1G. Recently, Sacristán et al. (2014) and Planellas et al. (2014) studied the effects of ultrasonic vibration on the material properties of micro-parts processed by an ultrasonic molding machine. In both cases, a 1000 W and 30,000 Hz ultrasonic generator coupled with a titanium alloy stepped sonotrode was used to melt the polymer pellets. They found that part morphology was highly dependent on processing conditions, as well as on the combination of process parameters required for Polylactide (PLA) and Polybutylene Succinate (PBS) material.

In this ultrasonic molding machine configuration (Sonorus 1G), the sonotrode has to be designed to vibrate in longitudinal mode (at a frequency determined by the generator). Otherwise, the sonotrode may collide with the plasticization chamber producing undesirable effects, such as deformation or cracks. Moreover it acts as a plunger and must be able to support all the forces and the heat generated during the melting process. The friction and the high temperatures can damage the sonotrode, wearing it down and altering the material properties; this can lead to the sonotrode frequency moving beyond the generator's vibration frequency range. This paper focuses on two issues concerning the sonotrode: (a) a design procedure to meet all the machine requirements, and (b) an analysis of the sonotrode life cycle from the point of view of wear.

The most commonly-used shapes in the design of sonotrodes are: cylindrical, tapered, stepped, exponential, conical and catenoidal. The German Electrical Manufacturers Association (1980) provides some theoretical and empirical equations to design and calculate preliminary dimensions of stepped and conical sonotrodes according to the required operating frequency and the material used. Nanu et al. (2011) presented a theoretical approach to design and simulate a stepped sonotrode used for ultrasonic assisted EDM with a copper electrode on the tip. They used simplified equations based exclusively on the material properties to calculate the sonotrode dimensions to vibrate at 20,000 Hz and then performed a FEM (finite element methods) analysis to determine the variation of sonotrode frequency regarding theoretical geometric variations. Their results showed that the frequency increases when the sonotrode mass decreases. Nad (2010) analyzed several sonotrode shapes (cylindrical, tapered, exponential and stepped) for ultrasonic machining technologies and characterized them by FEM to determine the resonance frequency and the transformation ratio. He found that the value of resonance frequency and the transformation ratio of a sonotrode are essential parameters for selecting suitable shapes which, in turn, are strongly related to the technological process under consideration. Wang et al. (2011) designed a new sonotrode to optimize the displacement amplification based on a cubic Bézier profile. They used a multi-objective optimization algorithm and a FEM analysis procedure to design it. Furthermore, they manufactured cylindrical Bézier sonotrode prototypes and compared their proposed design to experimental results using photonic sensors. The results were also compared to a catenoidal shape sonotrode to be used in ultrasonic cutting applications and they investigated the effects of the ultrasounds and sonotrode types on the penetration forces during this process. They compared the cutting forces with and without ultrasounds and the Beizer versus the and found that there was 50% higher displacement amplification and lower stress concentration for the Bézier profile. Considering these results, Wang and Nguyen (2014), designed a planar Bézier

catenoidal shape, and found that the Beizer profile provided higher amplification, while reducing the stress and penetration forces. Rani and Rudramoorthy (2013) studied the difference between different sonotrode shapes used in ultrasonic welding. The sonotrodes were simulated using FEM to evaluate their performance and they found that the maximum displacement was obtained with the Beizer and stepped profile, recording higher temperatures during the tests. Recently, Seo and Park (2012) designed a sonotrode to replicate micro-patterns in a polymer substrate by ultrasonic patterning.

The wear suffered by sonotrodes in ultrasonic molding has not yet been studied. The analysis carried out in this present research of several used sonotrodes provides a method of eliminating the presence of wear and its location in the sonotrode tip. According to Kumar (2013), tool wear in ultrasonic machining can be classified into two types: longitudinal wear and lateral/diametrical wear. It depends on several issues, such as process parameters or workpiece material, and is an important factor that affects process accuracy and performance. Only very small errors in setup or tool dimensions are allowable. In ultrasonic welding, sonotrode wear can appear when processing hard materials, such as liquid crystal polymers (Troughton, 2008). This effect can be increased when reinforced materials are processed, and it also occurs in machining processes (Palanikumar and Davim, 2009). Tool wear has also been studied in rotatory ultrasonic machining processes (Liang et al., 2012).

The literature shows that sonotrode design is inevitably linked to the end purpose of each technology and suggests that the steps taken during the design process are as follows: (a) a preliminary design is obtained using analytical equations to obtain a set of preliminary dimensions; (b) FEM modeling is then used to make adjustments according to vibration and machine requirements; (c) the sonotrode is manufactured; (d) experimental measurements are performed to validate the model and (e) the ultrasonic equipment is tested in order to check its performance. However, little attention has been paid to the effects of wear, which must also be considered to ensure the proper performance of the sonotrode during its life cycle. The novelty of the research presented in this paper is the two steps of the assessment (in this case, of a stepped sonotrode for ultrasonic molding technology): first, (a) apply the aforementioned design steps to predict the behavior of a stepped sonotrode during the ultrasonic molding process and then, (b) develop an operating frequencies map for the sonotrode according to the dimensional variations in the tip; this map can be used for re-designing new sonotrodes for the same job or for re-machining them, within certain limits, to extend their useful life.

2. Methodology

2.1. Methodology description

In ultrasonic molding, the acoustic unit consists of the transducer, the booster, the sonotrode and the generator (Fig. 2(a)). The electrical energy provided by the generator is converted into mechanical energy in the transducer. Vibration is then amplified by the booster and the sonotrode to obtain the desired vibration amplitude at the tip of the sonotrode. The design of the sonotrode in this case needs to take into account two main issues: (a) it must vibrate in longitudinal mode at the acoustic unit assembly

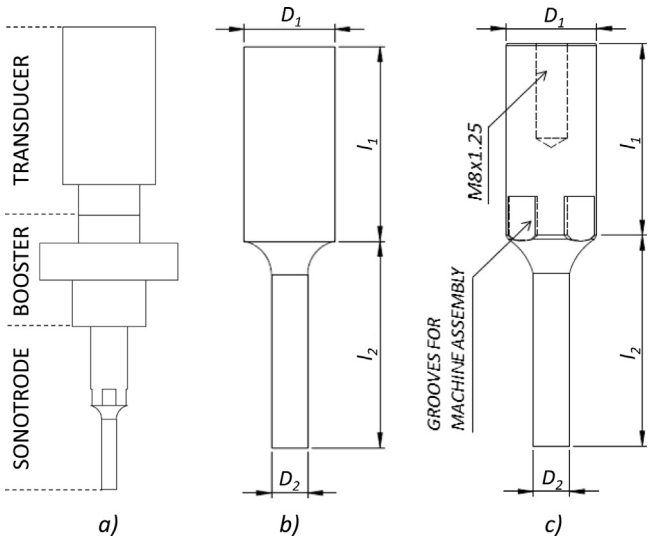

Fig. 2. (a) Components of the acoustic unit (b) theoretical geometry of a stepped sonotrode and (c) final sonotrode design having considered the machine requirements.

frequency of 30,000 ± 50 Hz, otherwise the sonotrode may collide with the plasticizing chamber during melting process, and (b) it must meet the specific design features which include holes, grooves, and specific diameter dimensions to fit it into the booster (Fig. 2(c)).

The design for the stepped sonotrode (Fig. 3) includes two main phases: the design approach and the FEM adjustments. In the design approach, analytical equations are used to obtain the preliminary stepped sonotrode dimensions (l_1, l_2, D_1, D_2). Next, based on these results, the CAD model is complemented with the specific design features required for its assembly into the acoustic unit and its final dimensions are adjusted by finite elements modeling software. The result is a FEM model of the sonotrode. For the FEM adjustment process, the diameter dimensions (D_1 and D_2) were fixed and then different combinations of lengths were tested until the sonotrode vibrated in a longitudinal mode nearest 30,000 Hz with maximum amplitude at its tip. This process was repeated until the combination of lengths achieved the longitudinal mode closest to 30,000 Hz. To validate the FEM model, an experimental analysis was carried out using the manufactured sonotrode (Fig. 3).

Taking into consideration the FEM model of the sonotrode and after analyzing several used sonotrodes from other work, a sonotrode operating frequencies map was created. The aim of this map is to find the maximum allowable variation of sonotrode length and tip diameter in order to increase the capacity for re-machining the sonotrode tip to remedy future wear.

2.2. Analytical, modeling and experimental procedure

This section explains in more detail each step described in Section 2.1.

2.2.1. Sonotrode design approaches

In this research, the stepped sonotrode (Fig. 2(b)) was designed in line with two analytical methods: (a) the ZVEI guidelines (ZVEI—German Electrical Manufacturers Association, 1980) and (b) Nanu et al. (2011). In any case the sonotrode needs to be designed to vibrate at 30,000 Hz to match the generator operating frequency. The titanium alloy used to make the sonotrode is Ti6Al4V, which has good strength, hardness and acoustic properties.

In stepped sonotrodes, according to the ZVEI guidelines (ZVEI—German Electrical Manufacturers Association, 1980), the

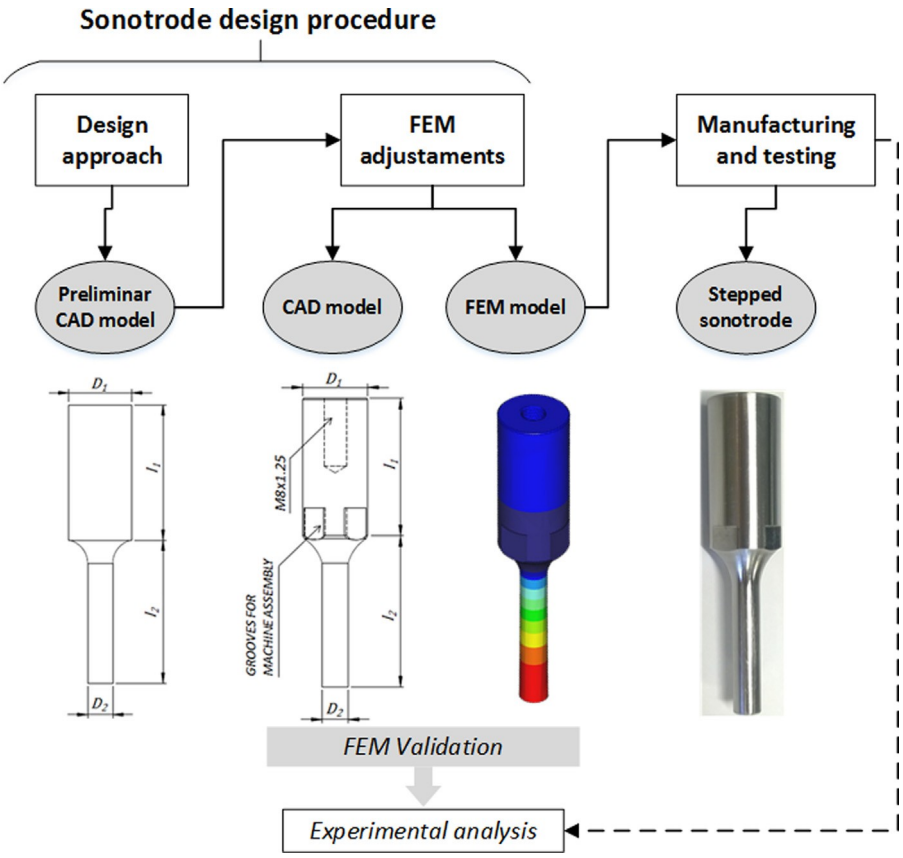

Fig. 3. Stages in the development of a stepped sonotrode for ultrasonic molding.

relationship between the two different diameters indicates the amplitude gain. For the sonotrode in this study, the input diameter – which is coupled to the booster – is 20 mm (D_1) while the output diameter – which is introduced into the plasticization chamber – is 8 mm (D_2). From this, a transformation ratio (K_t) of 6.25 was calculated using

$$K_t = \frac{\xi_1}{\xi_2} = \frac{A_1}{A_2} = \left(\frac{D_1}{D}\right)^2 \quad (1$$

where ξ_1 and ξ_2 represent the maximum vibration amplitudes on the input and output surfaces of the sonotrode, respectively; A_1 is the input surface area and A_2 is the output surface area. The vibration of 35 microns (ξ_2) on the tip of the sonotrode (i.e., maximum vibration on the output surface) is calculated as the combination of the gains of the transducer, the booster and the sonotrode.

The length of the sonotrode determines its resonance mode frequency. In this case, the combination of sonotrode lengths that guarantees a longitudinal vibrational mode at the desired frequency is theoretically calculated by the following equation: $l_0 = l_1 + l_2 = k_1 \frac{v}{4 \times f} + k_2 \frac{v}{4 \times f}$ (2)

where v is the sound velocity in the material, f is the frequency and k_1, *and* k_2 are coefficients that depend on the sonotrode cross sections. These values have been determined and adapted to the used working frequency by the method described in ZVEI Handbook (1980).

The sonotrode was then designed using the methodology developed by Nanu et al. (2011) who simplified Eqs. (1) and (2) and suggested the following expressions to determine the values of l_1 and l_2, as shown in Table 1:

$$l_1 = \frac{1.5}{k_u} \quad (3)$$

$$l_2 = \frac{1.6}{k_u} \quad (4)$$

where

$$k_u = \frac{2n}{} \quad (5)$$

$$= \frac{v}{f} \quad (6)$$

2.2.2. Sonotrode design based on computer modeling

A computer model based on FEM simulations was developed to adjust the sonotrode design approach (Fig. 2(b)) to the machine requirements by considering a threaded hole (M8 × 1.25) in the center of the top of the input surface and four semi-circular surface grooves on the sides of the output surface, as illustrated in Fig. 2(c).

To take these features into account, FEM software PTC Creo 2.0 was used to determine the final dimensions that provide a frequency value close to 30,000 ± 250 Hz in the longitudinal vibrational mode. The material properties used to run the computer simulations were a Young's modulus of 116.9 GPa, a density of 4453 g/cm^3 and a Poisson ratio of 0.33.

To determine the natural sonotrode vibration frequency, the following equation of motion is considered:

$$\boldsymbol{M}\ddot{\boldsymbol{d}} + \boldsymbol{K}\boldsymbol{d} = 0 \quad (6)$$

where $\boldsymbol{M}$ represents the global mass matrix, $\boldsymbol{K}$ describes the global stiffness matrix, $\boldsymbol{d}$ is the vector system displacement. To determine the system vibrational frequencies, it is assumed that the equation of motion satisfies the harmonic solution of the form:

$$\boldsymbol{d} = \cos\omega t \quad (7)$$

Table 1
Theoretical and final sonotrode dimensions.

Phase	Calculation method	l_1 (mm)	l_2 (mm)	$l_0 = l_1 + l_2$ (mm)	Frequency without requirements (Hz)	Frequency with requirements (Hz)
Design approach	ZVEI Handbook (1980)	42.47	44.53	87	29,608	29,742
	Nanu et al. (2011)	40.88	43.6	84.48	30,343	30,450
FEM adjustments	ZVEI Handbook (1980)	42,47	44.03	86.5	–	30,002
	Nanu et al. (2011)	40.88	44.36	85.24	–	29,997
	Final sonotrode design	42.94	45.41	88.35	–	30,023

where is a system parameter related to the mode shape (*i*th eigenvector), and ω is the natural frequency of the *i*th mode shape (*i*th eigenvalue). Substitution of Eq. (7) into Eq. (6), yields

$$-\boldsymbol{M}\ \omega\ ^2 cos\omega t + \boldsymbol{K}\ cos\omega t = 0. \quad (8)$$

Rearranging the terms, it is possible to show that the generalized eigenvalues can be determined from

$$\boldsymbol{K}\ =\ \boldsymbol{M} \quad (9)$$

where the substitution ω^2 is made in order to obtain the solution of Eq. (9) and to get the *n* system vibration frequencies, $\omega_i =$, with their corresponding free-vibration mode shapes, Geometric element analysis (GEA) was used and the structure was discretized into geometric elements. This mesh was divided into 1963 tetrahedral elements with 3221 edges and 4522 faces, with a minimum edge length of 10.04 mm and maximum edge angle of 167.86°. The boundary conditions were set in accordance with the sonotrode clamping conditions.

By using the computational model and by exciting the sonotrode at the frequency value of 30,000 Hz, the combination of sonotrode lengths are readjusted to activate the longitudinal vibration mode as well as to maximize the energy that is transmitted to the pellets during the manufacturing process.

2.2.3. Experimental analysis

Experimental measurements were carried out in order to validate the FEM model of the sonotrode. To obtain the dynamic behavior of the sonotrode, a non-contact laser vibrometer was used. The sonotrode vibrations were collected using a Polytec OFV 505 laser head and a Polytec™ OFV-5000 vibrometer controller. The frequency response functions of the ultrasonic molding unit were measured using a PCB 086C03 impact hammer. Vibrations signals were acquired through a 4-channel OROS OR35 vibration analyzer and the NVGate® 6.7 Noise and Vibration software platform. Fig. 4 shows the setup used for the experimental measurements.

The sonotrode was attached to soft elastic cords and suspended to perform the impact hammer test. For each collected frequency response function (FRF), a minimum of five impact tests were performed. The sonotrode was excited by the impact hammer at its largest diameter area in the longitudinal axis. The collected FRF showed the response of the system to the applied stimulus. In this particular case, laser vibrometer measured the velocity of the sonotrode (m/s) as a result of the impact force applied (N).

2.2.4. Analysis of the sonotrode life cycle

A set of previously used stepped sonotrodes (provided by the company that manufactured the ultrasonic molding machine) were analyzed in order to detect the presence and location of wear. These sonotrodes were also made of Ti6Al4 V and were selected from a set of sonotrodes used during the production of different polymeric components batches manufactured with acoustic units vibrating at 30,000 Hz. The processing conditions varied depending on the part material and geometry: the duration of ultrasonic energy applied in the working cycles was between 2 and 5 s, with amplitudes of vibration of up to 150 μm and an applied force of up to 6000 N. Although sonotrodes can withstand several working cycles, sometimes a bad alignment, or a tip buckling due to the applied force, can lead to contact between the sonotrode and the mold as the clearance between them is less than 0.1 mm. This can drastically accelerate sonotrode wear by friction (lateral wear). Tip wear is the result of the cyclical contact between sonotrode and polymer pellets, and it varies depending on each material. For this reason, sonotrode length and tip diameter were varied using the computational model and their corresponding longitudinal vibrational frequency values were determined. Increments of ±0.1 mm in the case of l_2 and 0.05 mm of D_2 were introduced into the FEM model to calculate a series of predicted vibration resonance values. In this way the maximum l_2 of the sonotrode at which it still vibrates within the lower limit of the operational vibration range (29,750 Hz) and the maximum possible reduction to this l_2 at which it will still function correctly in the upper limit (30,250 Hz) can be found. In the case of diameter, this reduction was applied only in the first 20 mm of the sonotrode tip, i.e., the part introduced into the plasticizing chamber during the molding cycle and which is susceptible to wear. With the obtained values, the operating frequency map of the sonotrode could be obtained.

3. Results

3.1. Sonotrode design procedure

Table 1 shows the results of the two design approaches and those of the computational model. The total variation of the sonotrode length (l_0) between the two analytical methods is 2.52 mm, being the sonotrode calculated using Nanu et al. (2011) equations shorter than the one obtained following the procedure detailed in ZVEI Handbook (1980). Theoretically, for a new sonotrode, both methods provided suitable dimensions to move to the stage of FEM adjustments.

Both sonotrodes approaches were simulated excluding the machine requirements (Table 1, column *Frequency without requirements*) and, in both cases, the frequency results were out of range. Nanu et al. (2011) approach is overcoming the upper frequency limit while ZVEI Handbook (1980) sonotrode is below the lower limit. Next, the machine requirements (the grooves and the thread) were added to the FEM models and, as expected, the mass reduction incremented the vibration frequency (Table 1, column *Frequency with requirements*). Finally, in both cases the lengths combination (l_1 and l_2) was adjusted. See the results in Table 1.

In this case, the dimensions that are closest to the real sonotrodes assembled in the SONORUS 1G machine correspond to those produced by the ZVEI Handbook (1980) method. Consequently, these dimensions were used for the final sonotrode design. As Table 1 shows, in the final design l_1 and l_2 were lightly adjusted to compensate the mass distribution to vibrate nearest to 30,000 Hz (ZVEI—German Electrical Manufacturers Association, 1980), due to quite mass was removed from D_1 zone.

For the final sonotrode design, there were twelve modal vibration frequencies whose values fall within the range of 20,000–35,000 Hz (Fig. 5). The longitudinal sonotrode vibrational mode occurs at the frequency value of 30,023 Hz (mode 8, Fig. 5(a)), and the maximum amplitude is observed at the tip of the sonotrode,

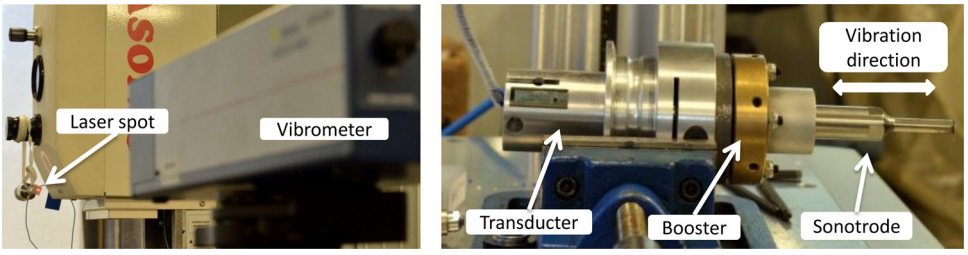

Fig. 4. Experimental setup for the sonotrode characterization with the Polytec OFV-5000 vibrometer.

Mode vibration		Frequency [Hz]
1		20571
2		22726
3		27319
4		27467
5		28141
6		28304
7	b	29007
8	a	30023
9	c	30823
10		31725
11		33814
12		33969

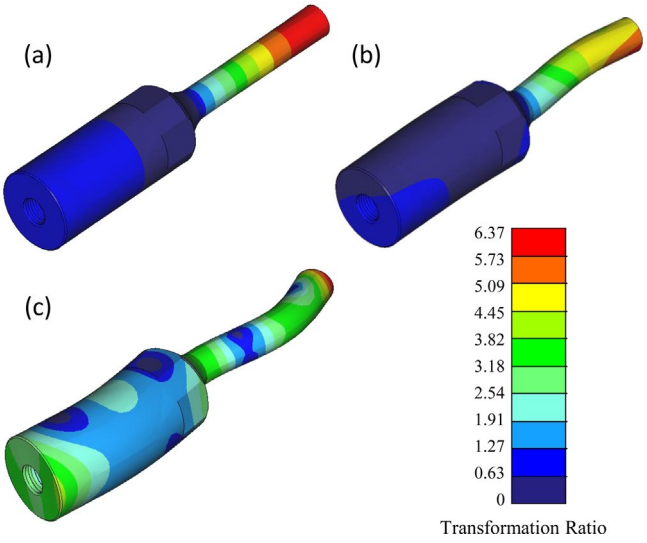

Fig. 5. Sonotrode vibration modes: (a) longitudinal mode (30,023 Hz), (b) twisting-longitudinal (29,007 Hz), and (c) twisting (30,823 Hz).

with a maximum gain of 6.37. Of course, other vibrational frequencies could be excited. Fig. 5 illustrates some of these other sonotrode vibrational modes which describe different physical behavior that is unsuitable for the ultrasound molding process. For instance, if the sonotrode is tuned to the operating frequencies of 29,007 Hz or 30,823 Hz, it will exhibit twisting behavior which could damage the mold and the sonotrode itself. Fig. 5(b) illustrates a twisting-longitudinal mode, while Fig. 5(c) shows a twisting vibrational mode.

3.2. Experimental analysis

The results of the experimental analysis are plotted in Fig. 6. Fig. 6(a) shows a typical sonotrode FRF (frequency response function) collected during the experimental impact hammer tests. From Fig. 6(a), it can be seen that the sonotrode exhibits vibrational modes at frequency values close to 30,000 Hz. In fact, the maximum peak value of the FRF occurs at frequency value of 30,045 Hz, which matches the acoustic unit working frequency. Fig. 6(b) compares the experimental results and the computed numerical values obtained from the computer simulation model. At the operating point, the experimental frequency peak value (30,045 Hz) is very close to the peak obtained from computer simulations (30,023 Hz) with a relative error smaller than 0.1%.

In addition, the dynamics performance of the whole acoustic equipment (Fig. 6(c)) was measured with the vibrometer system. In this case, the sonotrode was excited directly with the ultrasonic generator. The measured resonance frequency was 29,980 Hz which confirms that the sonotrode is oscillating near the design frequency value. As expected, this value differs from those previously discussed since this value corresponds to the acoustic unit array. In this particular case, experimental measurements showed that the sonotrode and the acoustic unit oscillate at frequency values close to the designed longitudinal operational frequency value of the sonotrode.

3.3. Analysis of the sonotrode life cycle

After analyzing several used stepped sonotrodes, it was found that some of them presented longitudinal (Fig. 7(a)) and lateral (Fig. 7(b)) wear. As shown in Fig. 7, usage marks are observed near the sonotrode tip, which corresponds with the part of the sonotrode that is introduced into the mold. The presence of wear indicates a mass variation at the tip of the sonotrode, which leads to a variation in the longitudinal vibration mode frequency. Moreover, the inhomogeneity at the worn surface causes a concentrated stress region and can lead to erroneous performance. In the particular case of Fig. 7(c), a rounded edge at the tip of the sonotrode is observed, which can cause a pressure drop in the molten polymer. Thus, in certain cases, eliminating the worn region can result in better performance and increase tool life. In the following sections, the results with regard to how dimensional variations on the sonotrode tip affect its dynamic response behavior are presented; specifically, with regard to the sonotrode length and the tip diameter variation.

3.3.1. Dynamic effect of the sonotrode dimensional variation

Two analysis were carried out with an initial length l_2 = 45.41 mm and a tip diameter D_2 = 8 mm, while l_1 and D_1 remained constant.

In the first analysis, length reductions of Δl_2 = 0.1 mm were introduced, keeping D_2 constant. Finite element simulations were used to determine the corresponding longitudinal vibration mode

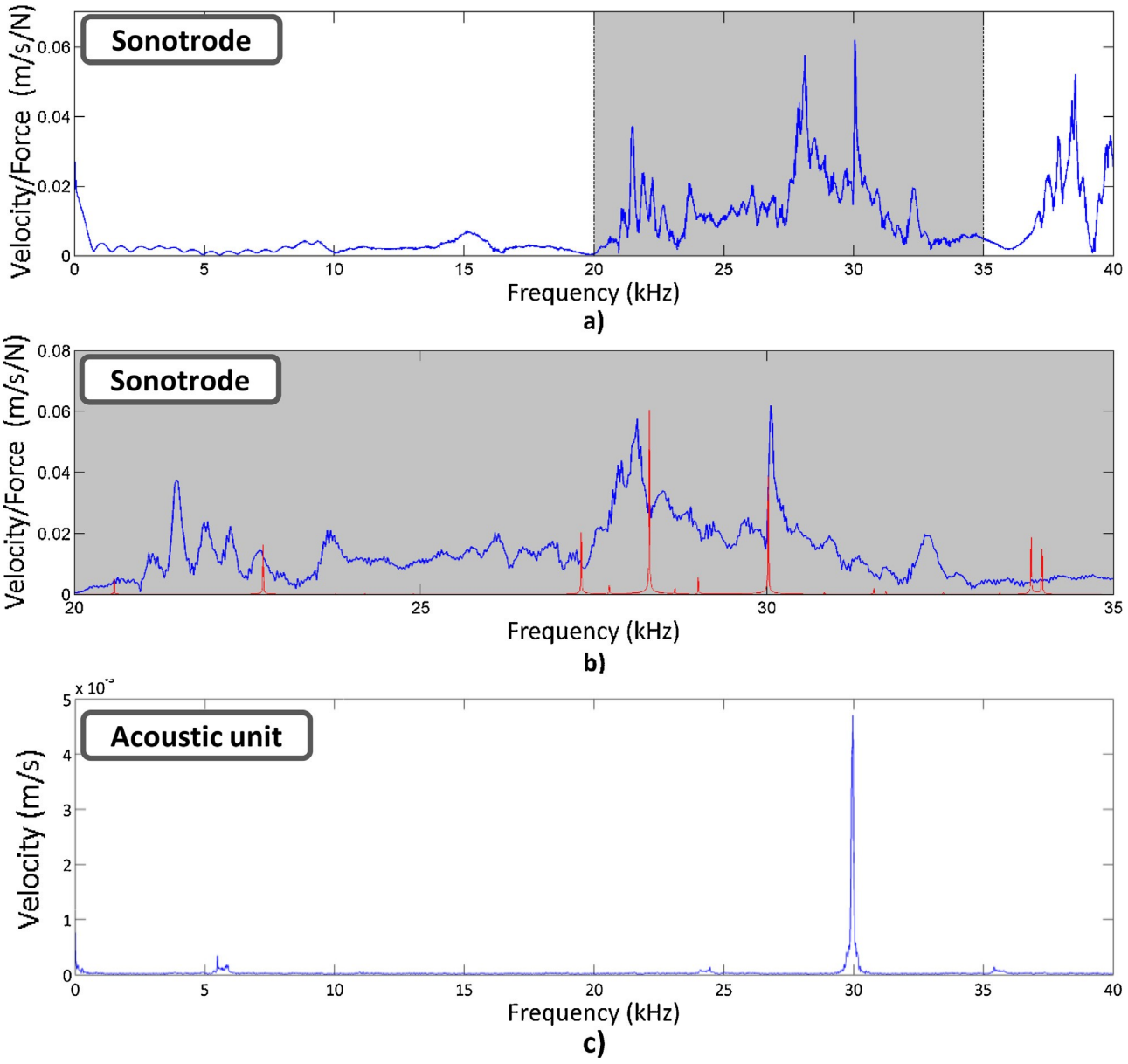

Fig. 6. Experimental vibrational response: (a) whole sonotrode frequency range, (b) 20,000–35,000 Hz amplification compared to simulation results (red solid lines) and (c) whole acoustic unit working response. (For interpretation of the references to color in this figure legend, the reader is referred to the web version of this article.)

frequencies. It was found that the length could be reduced to 45.11 mm, while keeping the longitudinal vibration mode within the operating range of 30,000 ±250 Hz (Fig. 8(a)). Exactly the maximum dimension, considering a linear trend, is 45,038 mm. This means that the sonotrode length could theoretically be re-machining 0.37 mm to eliminate wear and maintain the operating frequency of 30,250 Hz.

In the second analysis, the diameter was reduced with increments of $\Delta D_2 = 0.05$ mm at the tip of the sonotrode, keeping l_2 constant at 45.41 mm. In this case, it was found that the diameter could be reduced to 7.90 mm (Fig. 8(b)). The maximum diameter considering the lineal trend of the data is 7.89 mm vibrating in 30,250 Hz. This means the tip diameter could theoretically be re-machined by a maximum of 0.11 mm to eliminate wear and maintain the operating frequency.

The analysis of the dimensional variation showed that the resonance frequency value is increased when sonotrode length is reduced (Fig. 8(a)) and also when sonotrode tip diameter is reduced (Fig. 8(b)). In both cases, the reduction of mass in the tip of the sonotrode linearly increases the value of the resonance frequency of the longitudinal resonance mode.

The two analyses provide the range of dimensional variation that the sonotrode could theoretically undergo via re-machining and yet still function properly—thus extending its useful life. This range is, however, very narrow (0.37 mm in length and just 0.11 mm in diameter) and provides very little flexibility for re-machining a worn or defective sonotrode. This range can be extended by increasing the initial sonotrode tip length until it vibrates at the lower operational frequency limit of 29,750 Hz. The diameter cannot be increased due to the machine and mold constraints; however, the length of a new sonotrode can be increased.

Length increments of $\Delta l_2 = 0.1$ mm were introduced in the finite elements model to find the upper limit for sonotrode length that would maintain the longitudinal vibration mode of the sonotrode within the operational frequency range. This upper limit was found to be between 45.81–45.91 mm (Fig. 8(a)), concretely at 45.87 mm.

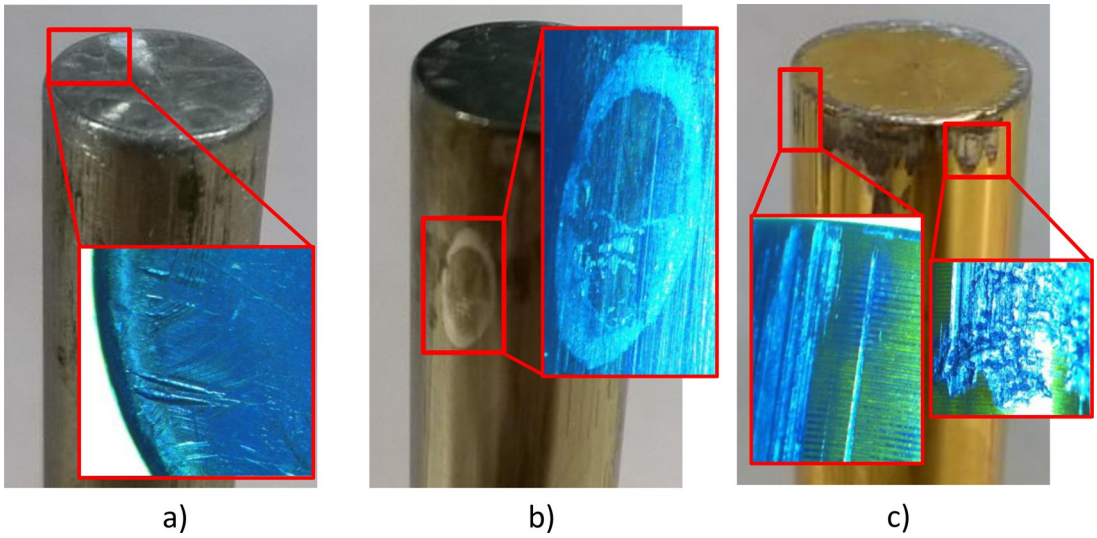

Fig. 7. Wear observed in different sonotrodes used in ultrasonic molding machines.

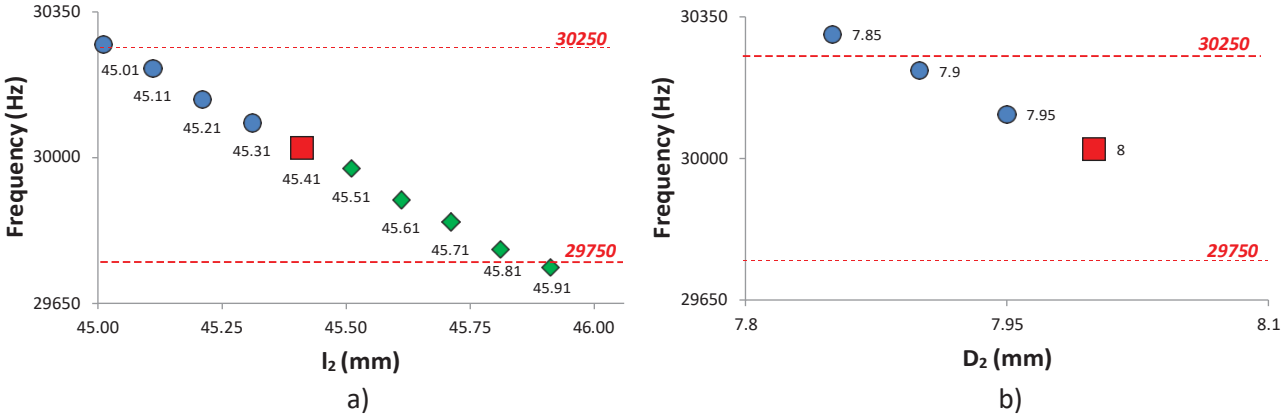

Fig. 8. Longitudinal vibration mode variation caused by dimensional variation (a) length reduction (b) tip diameter reduction.

This represents an increase of 0.456 mm, which extends the total dimensional range to 0.826 mm.

3.3.2. Operating frequencies map for a stepped sonotrode

The operating frequencies map of the sonotrode is obtained by combining the longitudinal vibrational frequencies predicted by varying the dimensions of l_2 and D_2. (Fig. 9). The red shaded cells show the range of l_2 and D_2 combinations that are produced by current sonotrodes designed to vibrate at 30,000 Hz. The white squares are combinations whose frequency values are beyond the upper operational limits. Finally, the blue squares show the functioning range in which an oversized sonotrode could work properly within operational limits.

This map can be used for two purposes: first, the functional life of a worn sonotrode can be extended using the dimensional limits provided by the map to re-machine it. Secondly, it can assist in the design of a new sonotrode. Any l_2 and D_2 combination that produces an operating frequency below the upper limit of 30,250 Hz and above the lower limit 29,750 Hz will produce a sonotrode whose acoustic system will function correctly. By designing it to vibrate as near as possible to the lower limit of 29,750 Hz, the sonotrode will have the maximum possible range of length and diameter available for re-machining after wear (i.e., the 'Design Region' in Fig. 9).

4. Discussion

Analytical models provide a good approximation of the sonotrode dimensions according to the desired resonance frequency. However, the equations of these models are based on simplified geometries and a FEM analysis for each particular case is required. In this study, both analytical approaches provide lengths combinations that vibrate near 30,000 Hz with longitudinal mode, but out of the operating range, therefore little adjustments were necessary.

Dimensional changes in the bigger diameter zone (D_1) have less effect over the modal frequency than the changes in smaller diameter (D_2) in stepped sonotrodes. The addition of the machine requirements, which affect the thicker part, modified the vibration frequency less than 150 Hz while a modification of 1 mm of the sonotrode tip length varied the frequency more than 500 Hz.

The differences between the experimental results, considering the manufactured sonotrode, and the FEM results may be caused to changes on the material properties of the raw material and machining accuracy. However around the objective frequency (30,000 Hz) less than 0.1 % error is achieved.

The result of the simulations showed that there is a lineal trend between the length and frequency variations, although several deviations can be detected in some points. Plotting the frequency

D_2 (mm) / L_2 (mm)	7.70	7.75	7.80	7.85	7.90	7.95	8.00
45.01	30887	30766	30698	30563	30470	30341	30272
45.11	30833	30709	30626	30501	30407	30281	30214
45.21	30770	30639	30566	30444	30342	30226	30139
45.31	30702	30583	30503	30386	30283	30165	30083
45.41	30648	30527	30443	30306	30217	30108	**30023**
45.51	30588	30467	30365	30241	30167	30048	29973
45.61	30527	30406	30300	30185	30104	29999	29898
45.71	30468	30319	30226	30130	30060	29937	29846
45.81	30408	30264	30169	30072	30002	29880	29780
45.91	30344	30209	30119	30015	29953	29820	29737
46.01	30289	30152	30047	29957	29885	29758	29658

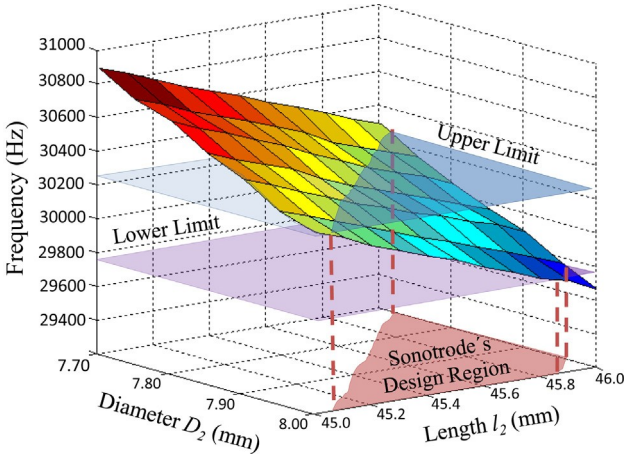

Fig. 9. Operating frequency map for designing a sonotrode and calculating tip re-machining range.

according to the length for each one of the simulated diameters (Fig. 9), linearity of the results is observed in all the cases. The maximum frequency error from the simulated points and the linear trend is below 25 Hz. The simulations also reveal that the longitudinal vibration mode is maintained in case the sonotrode needs to be machined due to wear effects. With the sonotrode readjusted, the distribution of masses along the longitudinal axes is constant. This is important, because the behavior of a sonotrode with a punctual defect is completely different and can lead to different vibration modes. The allowable range of dimensional variation is presented as a sonotrode operating frequencies map.

Temperature effects and interactions between the sonotrode and the polymer can influence the sonotrode behavior. Temperature variations due to the polymer melting temperature can change the material properties of the sonotrode, i.e., the elastic module, and alter its vibration frequency.

In the interaction sonotrode–polymer, the pushing force of the sonotrode can also affect the vibration frequency. The vibration recorded after several working cycles is not constant along the process. The frequency usually increases at the end of the process, when the sonotrode is submitted to the maximum force, to push the molten polymer to the cavity, and also when harder materials are processed. In both cases, the temperature of the sonotrode at the end of the cycle is increased, which can also influence on the results.

5. Conclusions

This paper has described how a sonotrode has to be carefully designed to ensure that its performance meets the machine and process requirements. Small variations in dimensions or shape, due to wear or cracks, have a strong influence on its dynamic performance.

A stepped sonotrode suitable for ultrasonic molding has been characterized. It was found that the longitudinal vibration frequency is inversely proportional with the dimensions of sonotrode tip. A reduction of the tip length produce an increase of the sonotrode vibration frequency, but the longitudinal vibration mode is still obtained.

An operating frequency map is a useful tool for adjusting the sonotrode dimensions – diameter and length – while maintaining vibration in a longitudinal frequency within the generator operational frequency range of 30,000 Hz ±250 Hz. Such a map can clearly identify the operating design region. This will produce a sonotrode with less restrictive tolerances; it will also be oversized in order to increase its useful life, assuming a fairly homogeneous wear pattern.

Future work should focus on investigating the impact of a variety of sonotrode shapes and dimensions, a more detailed study of the wear patterns of the sonotrode after several working cycles and extending this analysis by taking into account the effects of temperature, since temperature-induced variations in dimensions may modify the extreme limits of the frequency map.

Acknowledgements

The authors would like to express their gratitude to the following: ULTRASION SL for their support, assistance and close collaboration in this research, the department of Mechanical Engineering & Industrial Construction at the University of Girona and the *Consejo Nacional de Ciencia y Tecnología de México* (Conacyt), Project Number 242269. This project was carried out with the help of a DPI2013-45201-P reference grant awarded by the Spanish Government.

References

Kumar, J., 2013. Ultrasonic machining—a comprehensive review. Mach. Sci. Technol. 17 (3), 325–379.

Liang, Z., Wang, X., Wu, Y., Xie, L., Liu, Z., Zhao, W., 2012. An investigation on wear mechanism of resin-bonded diamond wheel in Elliptical Ultrasonic Assisted Grinding (EUAG) of monocrystal sapphire. J. Mater. Process. Technol. 212 (4), 868–876.

Liew, P.J., Yan, J., Kuriyagawa, T., 2014. Fabrication of deep micro-holes in reaction-bonded SiC by ultrasonic cavitation assisted micro-EDM. Int. J. Mach. Tools Manuf. 76, 13–20.

Michaeli, W., Kamps, T., Hopmann, C., 2011. Manufacturing of polymer micro parts by ultrasonic plasticization and direct injection. Microsyst. Technol. 17 (2), 243–249.

Michaeli, W., Opfermann, D., 2006. Ultrasonic plasticising for micro injection moulding. In: Menz, W., Dimov, S. (Eds.), Multi-Material Micro Manufacture. Grenoble, France, pp. 345–348.

Michaeli, W., Spennemann, A., Gärtner, R., 2002. New plastification concepts for micro injection moulding. Microsyst. Technol. 8 (1), 55–57.

Nad, M., 2010. Ultrasonic horn design for ultrasonic machining technologies. Appl. Comput. Mech. 4, 79–88.

Nanu, A.S., Marinescu, N.I., Ghiculescu, D., 2011. Study on ultrasonic stepped horn geometry. Design and FEM simulation. Nonconv. Technol. Rev. 15 (4), 25–30.

Palanikumar, K., Davim, J.P., 2009. Assessment of some factors influencing tool wear on the machining of glass fibre-reinforced plastics by coated cemented carbide tools. J. Mater. Process. Technol. 209 (1), 511–519.

Planellas, M., Sacristán, M., Rey, L., Olmo, C., Aymamí, J., Casas, M.T., del Valle, L.J., Franco, L., Puiggalí, J., 2014. Micro-molding with ultrasonic vibration energy: new method to disperse nanoclays in polymer matrices. Ultrason. Sonochem. 21 (4), 1557–1569.

Rani, R., Rudramoorthy, R., 2013. Computational modeling and experimental studies of the dynamic performance of ultrasonic horn profiles used in plastic welding. Ultrasonics 53 (3), 763–772.

Sackmann, J., Burlage, K., Gerhardy, C., Memering, B., Liao, S., Schomburg, W.K., 2015. Review on ultrasonic fabrication of polymer micro devices. Ultrasonics 56C, 189–200.
Sacristán, M., Plantá, X., Morell, M., Puiggalí, J., 2014. Effects of ultrasonic vibration on the micro-molding processing of polylactide. Ultrason. Sonochem. 21 (1), 376–386.
Sato, A., Ito, H., Koyama, K., 2009. Study of application of ultrasonic wave to injection molding. Polym. Eng. Sci. 49 (4), 768–773.
Seo, Y.-S., Park, K., 2012. Direct patterning of micro-features on a polymer substrate using ultrasonic vibration. Microsyst. Technol. 18 (12), 2053–2061.
Singh, R., Khamba, J.S., 2006. Ultrasonic machining of titanium and its alloys: a review. J. Mater. Process. Technol. 173 (2), 125–135.
Sirera, E., Plantá, X., Sacristán, M., 2012. USM®, nuevas oportunidades de negocio aplicando la tecnología de ultrasonidos al moldeo de mini / micro piezas de plástico de alta precisión. Rev. Plásticos Mod. Cienc. y Tecnol. los Polímeros, 176–180.
Tabatabaei, S.M.K., Behbahani, S., Mirian, S.M., 2013. Analysis of ultrasonic assisted machining (UAM) on regenerative chatter in turning. J. Mater. Process. Technol. 213 (2), 418–425.
Troughton, M.J., 2008. Handbook of Plastics Joining: A Practical Guide, 2nd ed. William Andrew, Norwich, NY.
Wang, D., Chuang, W.-Y., Hsu, K., Pham, H.-T., 2011. Design of a Bézier-profile horn for high displacement amplification. Ultrasonics 51 (2), 148–156.
Wang, D.-A., Nguyen, H.-D., 2014. A planar Bézier profiled horn for reducing penetration force in ultrasonic cutting. Ultrasonics 54 (1), 375–384.
Yang, Y.-J., Huang, C.-C., Lin, S.-K., Tao, J., 2014. Characteristics analysis and mold design for ultrasonic-assisted injection molding. J. Polym. Eng. 34 (7), 673–681.
ZVEI—German Electrical Manufacturers Association, 1980. Ultrasonic assembly of thermoplastic moldings and semi-finished products. Fachverband Electroschweissgera te, Frankfurt.